Heliyon 9 (2023) e20791

Contents lists available at ScienceDirect

Heliyon

journal homepage: www.cell.com/heliyon

Association of troponin I and macrophages in cardiac tamponade with Stanford type A aortic dissection

Satoshi Kimura [a,b,*], Hiroaki Sato [c], Shohei Shimajiri [b], Takahiro Umehara [c], Hirotsugu Noguchi [d], Daisuke Niino [e], Toshiyuki Nakayama [b]

[a] Department of Clinical Pathology, Kitakyushu City Yahata Hospital, Kitakyushu, Japan
[b] Department of Pathology, School of Medicine, University of Occupational and Environmental Health, Kitakyushu, Japan
[c] Department of Forensic Medicine, School of Medicine, University of Occupational and Environmental Health, Kitakyushu, Japan
[d] Department of Pathology, Field of Oncology, Graduate School of Medical and Dental Sciences, Kagoshima University, Kagoshima, Japan
[e] Pathology, Faculty of Medicine, Shimane University, Izumo, Japan

ARTICLE INFO

Keywords:
Aortic dissection
Cardiac tamponade
Chemokine
Macrophage
Troponin I

ABSTRACT

Background: Acute aortic dissection has a high mortality rate, especially for Stanford type A with a dissected ascending aorta. Cardiac tamponade is one of the most common complications of acute type A aortic dissection (ATAAD) and can cause death. However, the pathogenesis is often unclear. We aimed to examine laboratory findings at the onset of disease and macrophage involvement.

Methods: Hematological and biochemical parameters, and D-dimer, brain natriuretic peptide (BNP), and high-sensitivity troponin I (hs-cTnI) levels in 70 patients with ATAAD at our hospital were investigated. Additionally, the myocardium and aorta after autopsy of an ATAAD case with cardiac tamponade were pathologically examined.

Results: Forty-four ATAAD cases were complicated by cardiac tamponade. The mean age of patients with cardiac tamponade and proportion of patients over 70 years of age were both significantly higher than for those without cardiac tamponade. Evaluable D-dimer values were higher than 0.5 μg/mL in all patients. Significantly elevated laboratory parameters in patients with cardiac tamponade included: lactate dehydrogenase, aspartate aminotransferase, C-reactive protein, lactate, BNP, and hs-cTnI. However, multivariate analysis showed only hs-cTnI was significantly associated with cardiac tamponade. Histological examination revealed numerous M2-like macrophages infiltrating the myocardium and dissecting aorta, expressing CC chemokine ligand (CCL)2 together with vascular endothelial growth factor-C and matrix metalloproteinase-9. The peripheral monocyte-to-neutrophil ratio (MNR) was also significantly higher in cardiac tamponade.

Conclusions: In ATAAD patients with cardiac tamponade, hs-cTnI was significantly elevated and CCL2 expression was observed, which may be involved in the expression of M2-like macrophages via an increased MNR.

* Corresponding author. 2-6-2 Ogura, Yahatahigashi-ku, Kitakyushu, 805-8534, Japan.
E-mail address: s-kimura@med.uoeh-u.ac.jp (S. Kimura).

https://doi.org/10.1016/j.heliyon.2023.e20791
Received 20 November 2022; Received in revised form 8 September 2023; Accepted 6 October 2023
Available online 9 October 2023

1. Introduction

Acute aortic dissection is a disease that is occasionally encountered in the emergency room. In Japan, an average of 17.6 out of 100,000 people are affected annually, of which an average of 9.9 per 100,000 die. According to the Stanford classification system, acute aortic dissection is classified into type A, with dissection of the ascending aorta; the other is known as type B. Of these, acute Stanford type A aortic dissection (ATAAD) has an incidence of 64.2 %, while it accounts for 89.9 % of fatal cases [1]. Mortality rates reportedly increase over time so prompt diagnosis is essential [2].

In various countries, laboratory tests for the prognostic indicators of aortic dissection have been studied (e.g., D-dimer, peripheral neutrophil-to-lymphocyte ratio [NLR], C-reactive protein [CRP], and lactic acid, among others) [3]. In our previous study of patients with acute aortic dissection, we investigated the prognostic value of high-sensitivity troponin I (hs-cTnI) as a predictor of aortic dissection by investigating laboratory data and biomarkers related to the myocardium. High-sensitivity troponin I was significantly elevated in ATAAD compared to Stanford type B aortic dissection and was useful for a prognosis [4]. Cardiac tamponade is one of the major complications [5], and the most common cause of death, in ATAAD [6]. A complication of cardiac tamponade was thought to underlie a poor prognosis in ATAAD; however, its pathogenesis remains unclear. Macrophages are the predominant infiltrating cells in acute aortic dissection, and their role via the chemokine C–C motif chemokine ligand (CCL)2, a potent monocyte migration factor, has recently attracted attention [7]. In addition, macrophages are responsible for restoring tissue homeostasis through wound healing [8].

The early prediction of the complication of cardiac tamponade in ATAAD by laboratory data is quite difficult in the emergency room. We hypothesized that a significant increase of hs-TnI in ATAAD would be associated with the complication of cardiac tamponade. In this study, we assessed the utility of laboratory data, including hs-TnI, for predicting cardiac tamponade in ATAAD and examined the relevance of macrophages in this disease.

2. Materials and methods

2.1. Patients' backgrounds

Blood samples from 70 patients with ATAAD, taken when admitted to hospital between 2012 and 2022, were collected from the Kitakyushu City Yahata Hospital, Kitakyushu, Japan. The background of each patient in this study was as follows: a computed tomography scan confirmed dissection of the ascending aorta (mean inner diameter ± standard deviation [SD]: 44.97 mm ± 8.35). Patient samples (females, 40; males, 30; aged 41–94 years average ± SD: 73.87 ± 14.21) were obtained at diagnosis. Of these patients, 38 (54.3 %) had known hypertension (Table 1) and two (2.9 %) had diabetes. Patients with known connective tissue disease causing aortic dissection, acute infectious conditions, non-compensated liver disease, or acute myocardial infarction status by evaluable electrocardiograph were excluded.

These retrospective, research-related examinations were conducted in accordance with the guidelines of the Declaration of Helsinki and were approved by the Research Ethics Committee of the Kitakyushu City Hospital Organization (permission number: 202112001).

2.2. Laboratory data on admission

Lactate dehydrogenase (LD), aspartate aminotransferase (AST), creatine kinase (CK), C-reactive protein (CRP), white blood cell count (WBC), peripheral NLR, lactate, D-dimer, brain natriuretic peptide (BNP), and hs-cTnI were measured by blood collection immediately after each patient's visit. The following instruments were used: XN-2000 (Sysmex, Kobe, Japan) for blood tests; BioMajestyJCA-BM6070 (JEOL, Tokyo, Japan) and JCA-BM6010 (JEOL) for biochemistry tests; RADIOMATERABL90 FLEX for lactate; and Coapresta CP3000 (Sekisui Medical, Tokyo, Japan) and CS-2000i (Sysmex, Kobe, Japan) for coagulation tests. Brain natriuretic peptide and hs-cTnI were measured by PATHFAST (LSI Medience Corporation, Tokyo, Japan) using plasma; measurement ranges were 4∼2000 pg/mL and 0.02–50 ng/mL, respectively. Two instruments (Coapresta CP3000 and CS-2000i) were used for D-dimer measurements. A correlation test at our institution showed that Y(CP3000) = The correlation test at our hospital, which showed that Y (CP3000) = 0.6369× (CS-2000i) + 0.493, r = 0.9838, and X was converted to Y (measurement range: 0.5–60 μg/mL). The normal

Table 1
Characteristics of patients with acute aortic dissection.

Parameters	Tamponade (+)	Tamponade (−)	Total	*P*-value
No. of patients (total%)	44 (62.9 %)	26 (37.1 %)	70	
Mean age ± SD, years (range)	77.23 ± 13.40 (47–94)	68.19 ± 13.95 (41–94)	73.87 ± 14.21 (41–94)	0.011*
Age (>70 years)	31 (75.6 %)	10 (38.5 %)	41 (58.6 %)	0.012*
Gender (female)	27 (61.4 %)	13 (50.0 %)	40 (57.1 %)	0.455
History of hypertension	20 (45.5 %)	18 (69.2 %)	38 (54.3 %)	0.082
Aortic rupture	6 (13.6 %)	6 (23.1 %)	12 (17.1 %)	0.341
Death within 24 h	36 (81.8 %)	6 (23.1 %)	42 (60.0 %)	<0.001***
D-dimer (>0.5 μg/mL)	15/15	15/15	30/30	–
Mean inner diameter of ascending aorta ±SD, mm	45.25 ± 8.46	44.51 ± 8.30	44.97 ± 8.35	0.721

SD: standard deviation. For parameters that could not be evaluated in all cases, the denominator is listed as the number of cases surveyed. *$p < 0.05$ and ***$p < 0.001$.

reference ranges for these assays are summarized in Table 2. Hemolyzed samples were excluded from biochemical and D-dimer tests.

2.3. Histopathological stains

Aortic and myocardial samples were obtained from the autopsy of an 85-year-old man with ATAAD in whom aortitis syndrome, an autoimmune disease, or coronary artery occlusion were ruled out. Conservative treatment was chosen at the patient's request but he died 3 days after admission due to cardiac tamponade complications. This case was an autopsy case with a clear time course from the onset of ATADD to the complication of cardiac tamponade.

After fixation of tissues in 10 % formalin and embedding in paraffin, tissue sections (3-μm thick) underwent hematoxylin and eosin, Azan, and Elastica van Gieson (EVG) staining.

2.4. Immunohistochemical analysis

Tissues were fixed with 10 % formalin and embedded in paraffin. Sections (4-μm thick) were used for immunohistochemical examinations with an Histostainer 36A automated immunostainer (Nichirei Biosciences Inc., Tokyo, Japan). Mouse monoclonal antibodies against human CD68 (clone KP1, 1:100), histidine decarboxylase (HDC; 1:100), and α-smooth muscle actin (SMA; clone1A/4, 1:100) were obtained from Dako (Kyoto, Japan). Mouse monoclonal antibody against human CD163 (clone 10D6, 1:100) was from Leica (Tokyo, Japan) and mouse monoclonal antibody against D2-40 (clone D2-40, 1:1) was from Nichirei (Tokyo, Japan). Rabbit polyclonal antibodies to CCL2 (1:200) and CCL22 (1:100) were obtained from Abcam (Tokyo, Japan). Rabbit polyclonal antibody to HDC (1:200) was obtained from Progen Biotechnik (Heidelberg, Germany).

2.5. Immunofluorescence examinations

Immunofluorescence examinations were performed on 4-μm thin sections using rabbit polyclonal anti-human CCL2 from Abcam (1:200; Tokyo, Japan). Mouse monoclonal antibody against human complement component (C) 9 (53, 1:50) was from Abcam (Tokyo, Japan). Mouse monoclonal antibody against vascular endothelial growth factor (VEGF)-C (MM0006-2E65, 1:50) was from Novus Biologicals (Centennial, CO, USA). Mouse monoclonal antibody against matrix metalloproteinase (MMP)-9 (E11, 1:100) was obtained from Santa Cruz (Dallas, Texas, USA). Rhodamine-conjugated goat anti-rabbit IgG (H + L; 1:200; Merck, Tokyo, Japan) or fluorescein isothiocyanate (FITC)-conjugated goat anti-mouse IgG (H + L; 1:200; Merck) were used as secondary antibodies. A 6-diamidino-2-phenylindole (DAPI; GeneTex, Hsinchu City, Taiwan) stain was used as a nuclear stain. Immunofluorescent sections were observed with a Nikon ECLIPSE E600 inverted fluorescence microscope (Nikon, Tokyo, Japan) and analyzed by LuminaVision software (version 2.2.2; Mitani Corporation, Tokyo, Japan).

2.6. Statistical analysis

Statistical analyses of data between groups were performed using Welch's *t*-test, a Brunner–Munzel test, and Fisher's exact test, respectively. Odds ratios and corresponding 95 % confidence intervals were calculated from multiple imputation methods to address missing data (data set: m = 20, analysis software: mice ver. 3.13.0). All *p*-values <0.05 were considered statistically significant. All statistical analyses were performed using the R commander (The R Foundation for Statistical Computing, Vienna, Austria, version 3.6.1) designed to add statistical functions frequently used in biostatistics. Lactate, hs-cTnI, and BNP levels were validated using cut-off scores based on the results of a receiver operating characteristic (ROC) curve analysis to define the optimum cut-off value.

Table 2
Overview of normal reference ranges for laboratory data.

Parameters		Lower limit	Upper limit	Unit
LD		124	222	U/L
AST		13	30	U/L
CK	female	41	153	U/L
	male	59	248	
CRP		0.00	0.14	mg/dL
WBC		3.3	8.6	$\times 10^3/\mu L$
Lactate		0.5	1.6	mmol/L
D-dimer		–	≤1.0	μg/mL
BNP		–	≤19.5	pg/mL
hs-cTnI		–	≤0.028	ng/mL

AST: aspartate aminotransferase, BNP: brain natriuretic peptide, CI: confidence interval, CK: creatine kinase, CRP: C-reactive peptide, hs-cTnI: high-sensitivity troponin I, LD: lactate dehydrogenase, WBC: white blood cell count.

3. Results

3.1. Characteristics of ATAAD cases complicated by cardiac tamponade

The mean age of patients with cardiac tamponade was significantly higher than that of patients without cardiac tamponade. Significantly more patients with cardiac tamponade were also over 70 years of age, which is considered a high risk for developing aortic dissection. In addition, the mortality rate within 24 h was significantly higher in patients with cardiac tamponade (Table 1). These findings suggest that increased age is a risk factor for developing cardiac tamponade and subsequent death. In comparison, no significant difference was noted with regard to a history of hypertension and the mean inner diameter of the ascending aorta between the two patient groups (Table 1).

3.2. Comparison of laboratory data of blood samples from patients with and without cardiac tamponade complications

General biochemical tests in patients with ATAAD showed significantly elevated LD, AST, and CRP levels in those with cardiac tamponade complications (Fig. 1A, B, and D, respectively). In contrast, no significant difference was noted in the CK level between those with and without cardiac complications (Fig. 1C). For leukocytes, no significant differences in the WBC and NLR were found between the two ATAAD patient groups (Fig. 1E, and F, respectively).

Significant differences were observed in lactate, BNP, and hs-cTnI levels (Fig. 2A, C, and D, respectively) for ATAAD cases with and without cardiac tamponade complications. No significant differences were found between these two patient groups for the results of the D-dimer test, which is commonly used to diagnose aortic dissection (Fig. 2B). The ROC curves for lactate, D-dimer, BNP, and hs-cTnI were 0.757, 0.624, 0.764, and 0.834, respectively, with hs-cTnI having the highest value (Fig. 2-ROC). Thus, LD, AST, and CRP levels, as well as lactate, BNP, and hs-cTnI levels, were significantly increased in ATAAD patients with cardiac tamponade

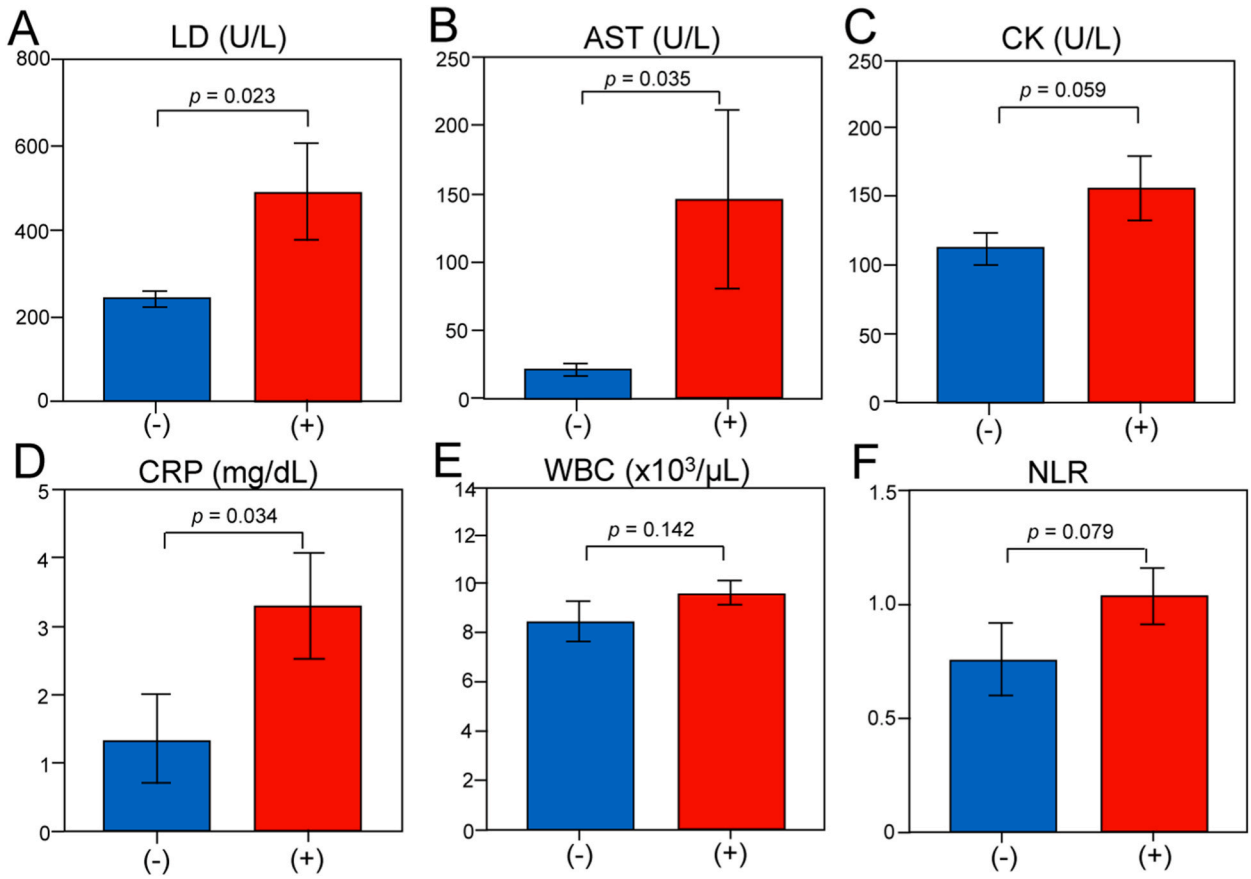

Fig. 1. Biochemistry and blood count data findings on admission
Lactate dehydrogenase (LD), aspartate aminotransferase (AST), creatine kinase (CK), C-reactive protein (CRP), white blood cell counts (WBC), and peripheral neutrophil-to-lymphocyte ratios (NLR) were compared in Stanford type A aortic dissection (ATAAD) cases, with and without cardiac tamponade complications. Mean values for LD, AST, and CRP were significantly increased in patients with cardiac tamponade complications ($p = 0.023$, $p = 0.035$, and $p = 0.034$, respectively; Figures A, B, and D).
These statistical analyses were based on one-sided tests.

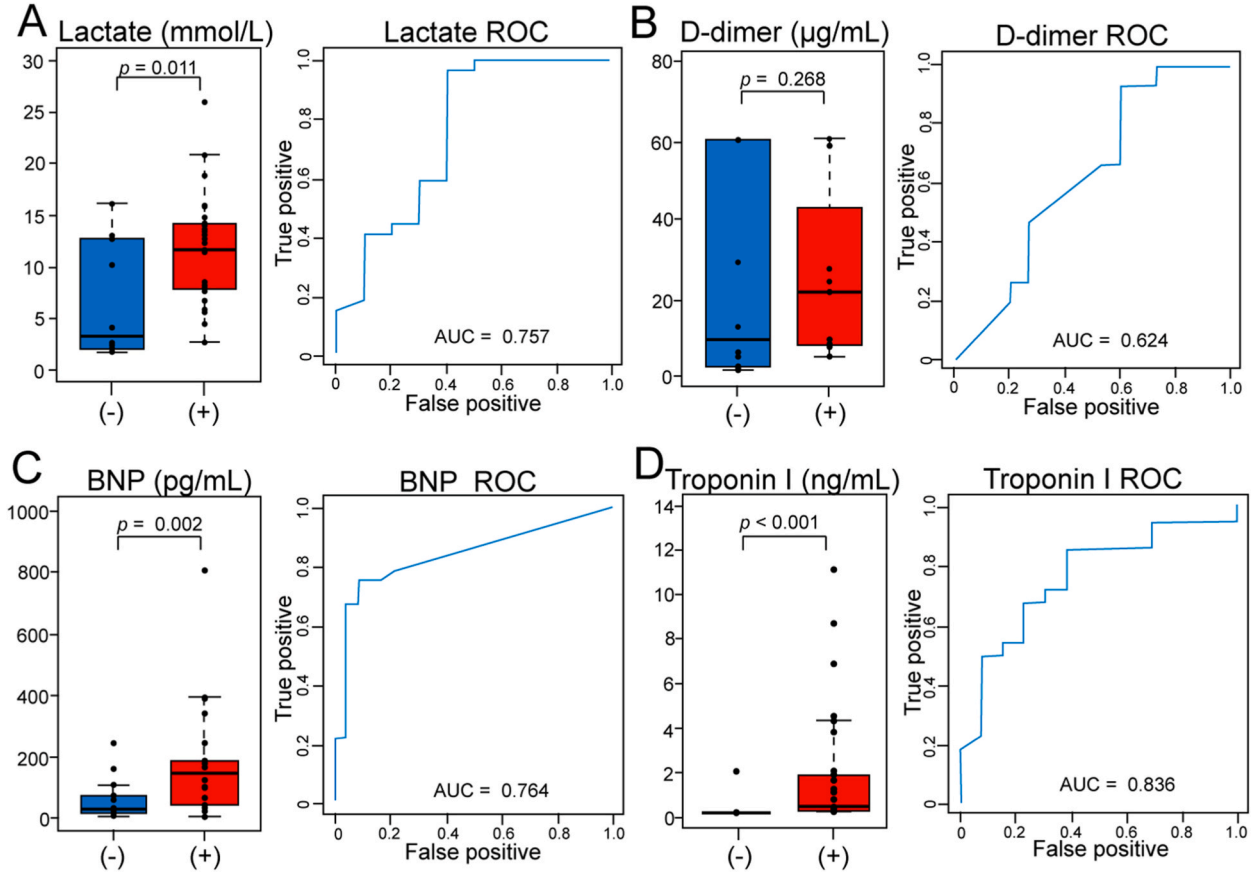

Fig. 2. Lactate, D-dimer, and cardiac biomarker findings Lactate, D-dimer, brain natriuretic peptide (BNP), and high-sensitivity troponin I (hs-cTnI) were compared in Stanford type A aortic dissection (ATAAD) cases, with and without cardiac tamponade complications. Receiver operating characteristic (ROC) curves were developed for determining cut-off values. The central tendencies of lactate, BNP, and hs-cTnI were significantly increased in patients with cardiac tamponade complications ($p = 0.0011$, $p = 0.002$, and $p < 0.001$, respectively; Figures A, C, and D, respectively). The areas under the curve (AUCs) for lactate, D-dimer, BNP, and hs-cTnI by ROC curve were 0.757, 0.624, 0.764, and 0.836, respectively (Figures A-, B-, C-, and D-ROC). Horizontal bars represent the 10th to 90th percentile range, and boxes indicate the 25th to 75th percentile range. The horizontal lines in each box correspond to the median.
These statistical analyses were based on one-sided tests.

Table 3
Univariate and multivariate analyses used to identify independent predictors for a diagnosis of Stanford type A acute aortic dissection with cardiac tamponade.

Parameters		Tamponade		Univariate				Multivariate			
				OR	95 % CI		*P*-value	OR	95 % CI		*P*-value
		(+)	(−)		lower	higher			lower	higher	
LD (U/L)	>222	37	11	1.811	0.440	7.445	0.399				
	≤222	11	7								
AST (U/L)	>30	8	3	11.720	1.949	70.478	0.009**	1.430	0.044	45.962	0.830
	≤30	11	15								
CRP (mg/dL)	>0.14	18	1	1.896	0.538	6.690	0.310				
	≤0.14	8	14								
hs-cTnI (ng/mL)	≥0.025	30	3	28.667	5.684	144.584	<0.001***	13.429	1.164	154.873	0.038*
	<0.025	7	20								
BNP (pg/mL)	≥32.7	19	5	6.831	1.573	29.659	0.012*	4.584	0.532	39.478	0.160
	<32.7	3	8								
Lactate (mmol/mL)	≥2.8	27	5	13.462	1.219	148.713	0.036*	3.648	0.097	137.751	0.456
	<2.8	0	5								

AST: aspartate aminotransferase, BNP: brain natriuretic peptide, CI: confidence interval, CRP: C-reactive peptide, hs-cTnI: high-sensitivity troponin I, LD: lactate dehydrogenase, OR: odds ratio: *$p < 0.05$, **$p < 0.01$, and ***$p < 0.001$.

complications.

These significant factors were analyzed by univariate and multivariate analyses. We used the upper limit of standard reference intervals as cut-off values for tests (LD, AST, and CRP; Table 3). We used the cut-off values calculated from ROC curves for tests without reference intervals (hs-cTnI, BNP, and lactate; Table 3). Univariate analysis showed significant differences in AST, hs-cTnI, BNP, and lactate levels ($p = 0.009$, $p < 0.001$, $p = 0.012$, and $p = 0.036$, respectively) between ATAAD cases with and without cardiac tamponade complications. Furthermore, when these factors were analyzed in a multivariate analysis only hs-cTnI ($p = 0.038$) was an influential factor affecting cardiac tamponade complications (Table 3). Thus, ATAAD with cardiac tamponade was associated with increased hs-cTnI.

3.3. Relationship between aortic dissection and macrophages

Macrophages have a variety of roles with respect to wounds. We investigated the function and differentiation of macrophages involved in vascular wall injury due to aortic dissection to evaluate any associations between laboratory data.

Fig. 3A shows the edge of the dissection. Smooth muscle and collagen fibers were observed with tears (Fig. 3A-EVG and -SMA) but were not completely dissected. Partial granulation tissue (Fig. 3A-HE high-power) was observed that was surrounded by macrophage infiltration (Fig. 3A-CD68). Around the macrophages, vascular vessel growth was observed (Fig. 3A-CD34) some of which was positive for D2-40 (Fig. 3A-D2-40).

Fig. 3B shows a portion of a complete dissection. In the dissected aortic tunica media, elastic fibers were completely ruptured and smooth muscle was fragmented (Fig. 3B-EVG and -SMA). Numerous macrophages were seen in the dissociated tunica media and false lumen (Fig. 3B-CD68). Macrophages in Fig. 3A and B were positive for CD163 and CCL22, markers of M2-like macrophages (Fig. 3A-, 3B-CD163, and CCL22). In addition, HDC-positive macrophages (Fig. 3B-HDC) and macrophages showing the phagocytosis of iron (Fig. 3B-Berlin blue) were also observed. The lesions showed a large number of CCL2-positive cells that co-expressed VEGF-C and MMP-9 (Fig. 3A-VEGF-C and 3B-MMP-9). Thus, M2-like macrophages were found to be frequently present and expressed a variety of molecules in acute aortic dissection lesions.

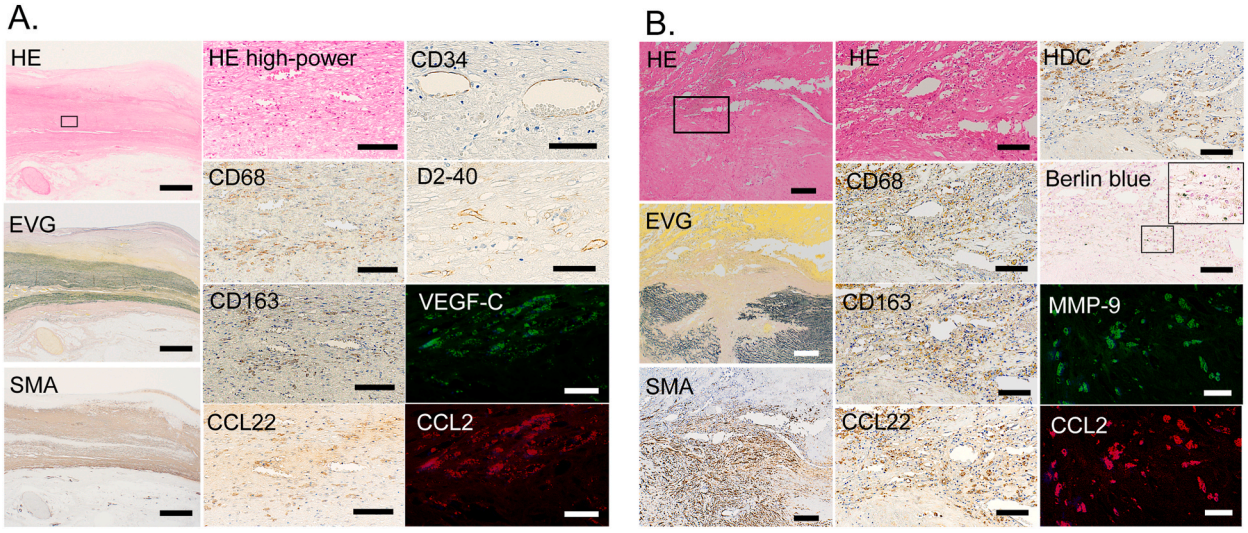

Fig. 3. Expression of macrophages in Stanford type A aortic dissection tissue

Figures A and B show the edge of a dissection and a completely dissected portion of Stanford type A aortic (ATAAD) tissue, respectively. In Figure A, complete detachment of the media is not evident, but obscuration of the smooth muscle and breakage of the elastic fibers are observed (A-EVG and -SMA). Figure A-HE high power is derived from the inset of Figure A-HE. Figures A-CD68, -CD163, and -CCL22 show the same sites as in Figure A-HE high power. Figures A-CD34 and -D2-40 show vascularized areas of the media. Aggregation sites of CD68-positive cells were fluorescently stained with anti–VEGF-C (green) and -CCL2 (red) (A-VEGF-C and -CCL2) antibodies.

In Figure B, the elastic fibers of the complete aortic media were completely dissected and smooth muscle showed fragmentation (B-EVG and -SMA). Figure B-HE high power is derived from the inset of Figure B-HE. Figures B-CD68, -CD163, -CCL22, -HDC, and -Berlin blue show the same sites as in Figure B-HE high power. The inset of the B-Berlin blue image shows a high-power magnification of the smaller inset. Aggregation sites of CD68-positive cells were fluorescently stained with antibodies against MMP-9 (green) and CCL2 (red) (A-MMP-9 and -CCL2). Blue (DAPI) indicates the nuclei of cells.

Scale bars: 1 mm in A-HE, -EVG, and -SMA; 200 μm in B-HE, -EVG, and -SMA; 50 μm in A and B-HE high power, -CD68, -CD163, -CCL22, A-CD34, A-D2-40, B-HDC, and -Berlin blue; 10 μm in A and B-CCL2, A-VEGF-C, and B-MMP-9.

CCL, C–C motif chemokine ligand; DAPI, 6-diamidino-2-phenylindole; EVG, Elastica van Gieson; HE, hematoxylin eosin; HDC, L-histidine decarboxylase; MMP, matrix metalloproteinase; SMA, α-smooth muscle actin; VEGF, vascular endothelial growth factor.

3.4. Relationship between myocardium and macrophages in Stanford type A aortic dissection with cardiac tamponade

The CCL2 expressed by macrophages plays an important role in the myocardium via monocyte migration. Myocardial status and macrophage expression were examined to evaluate the elevated hs-cTnI level.

Fig. 4A-HE shows the myocardium with tamponade, mechanical fragmentation of the myocardium, and inflammatory cell infiltration into the stroma. Scattered contraction band necrosis was observed in the myocardium under high-power magnification (Fig. 4A-HE high-power and -Azan). Cardiomyocytes were observed to be partially positive for C9 and simultaneously expressed CCL2 (Fig. 4A-C9 and -CCL2). Macrophages were positive for CCL2 (Fig. 4A-CCL2; arrowheads). Inflammatory cells in the stroma were predominantly CD68-positive macrophages, which were also positive for CD163 and CCL22 (Fig. 4A-CD68, -CD163, and -CCL22). Histidine decarboxylase–positive cells were found in the intravascular and perivascular areas of the stroma (Fig. 4A-HDC). $CD68^{-}$and CD163-positive macrophages were also distributed in the interstitial and perivascular space, endocardial endothelium, and endocardium and epicardium (Fig. 4B-CD68 and -CD163). Hence, our findings suggest that cardiomyocytes expressed CCL2 and many M2-like macrophages infiltrated the heart in ATAAD with cardiac tamponade.

3.5. Troponin I and aspartate aminotransferase to lactate dehydrogenase ratio

AST and LD are elevated simultaneously in a variety of diseases, whereas the ratio of elevation depends on the characteristics of the disease. Mean values of AST and LD were also significantly increased in ATAAD patients with cardiac tamponade ($p = 0.023$ and $p = 0.035$), with AST and LD being about 6.43 and 2.00 times higher, respectively, than in ATAAD patients without cardiac tamponade (Fig. 1A and B). This resulted in a more pronounced and significant difference when comparing the AST/LD ratio between ATADD patients with and without cardiac tamponade ($p < 0.001$: Fig. 5A). In a new attempt, we investigated the correlation between troponin I and the AST/LD ratio, and the similarity of elevation between troponin I and AST/LD ratios. Troponin I and the AST/LD ratio were found to be significantly correlated ($r = 0.601$, $p = 0.039$: Fig. 5B). Accordingly, ATAAD with cardiac tamponade was associated with an increased AST/LD ratio.

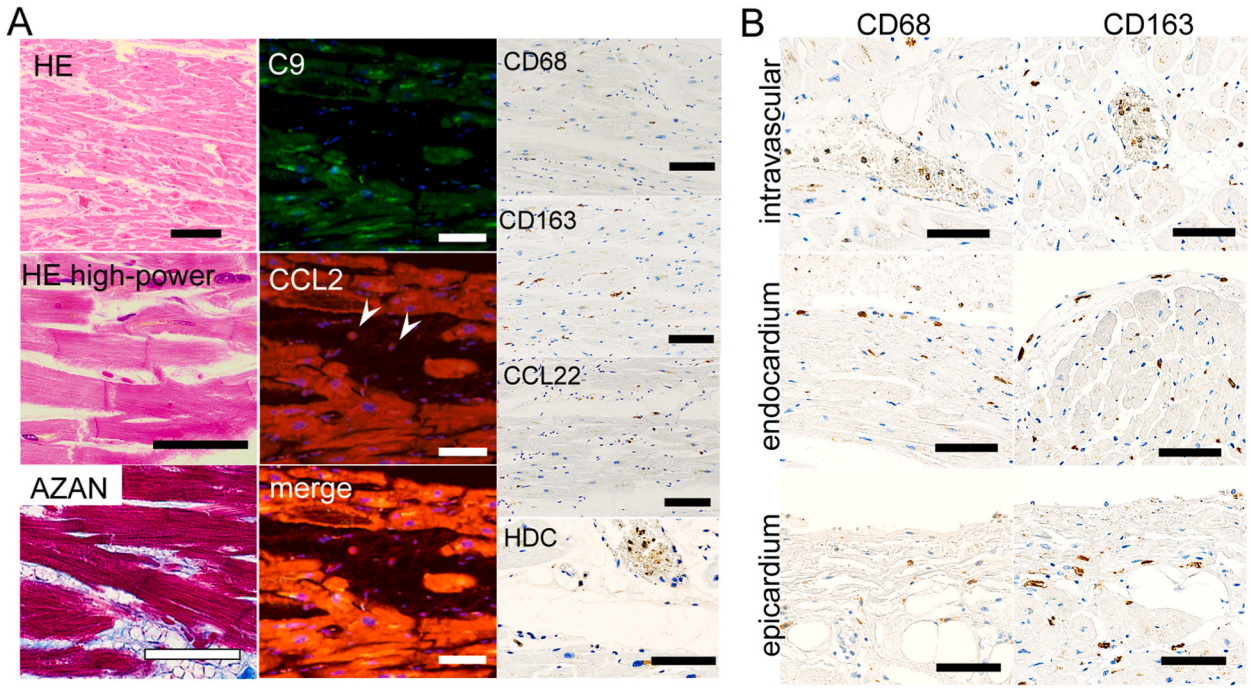

Fig. 4. Histological findings and expression of macrophages in the myocardium of patients with cardiac tamponade
Figure A shows histological findings of the myocardium, including the expression of macrophages in myocardial tissue. A-HE high power and -Azan were high-power magnified images of myocardial fibers with fragmentation and rupture showing contraction band necrosis.
Immunofluorescence staining showed C9 (green: A-C9), CCL2 (red: A-CCL2), and a merged image of these (A-merge). Arrowheads indicate CCL2-positive macrophages.
Figure Bshows the localization of $CD68^{-}$and CD163-positive monocytes/macrophages in intravascular vessels, pericardial endocardium, and epicardium of the myocardium.
Scale bars: 500 μm in A-HE; 100 μm in A-CD68, -CCL22, and -CD163; 50 μm in A-HDC and B; 20 μm in A-HE high power, -Azan, -C9, -CCL2, and -merge.
C9, complement component 9; CCL, C–C motif chemokine ligand; HDC, L-histidine decarboxylase; HE, hematoxylin eosin.

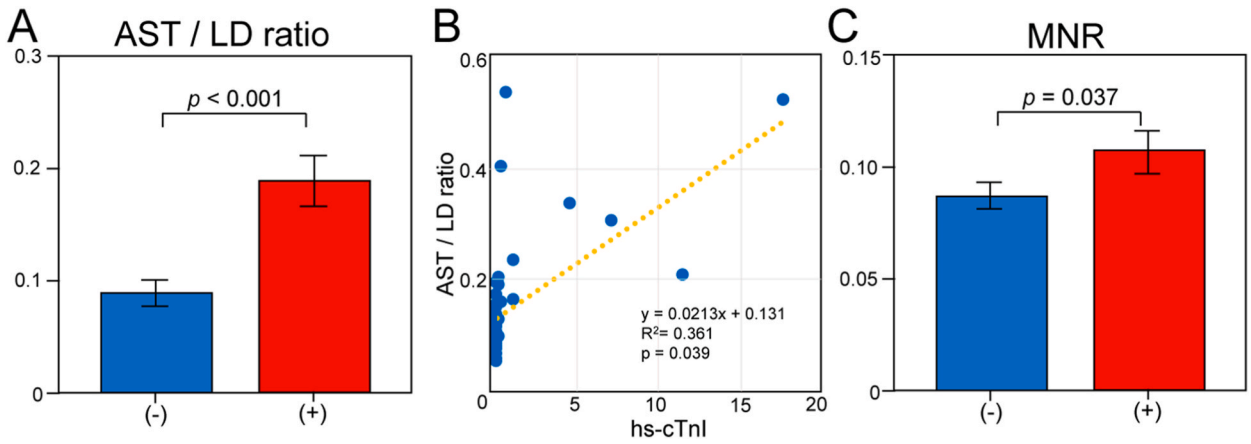

Fig. 5. Aminotransferase to lactate dehydrogenase ratio and monocyte-to-neutrophil ratio.
Figure Ashows the relationship between the aspartate aminotransferase (AST) to lactate dehydrogenase (LD) ratio and cardiac tamponade. Figure B shows the correlation between the AST to LD ratio and high-sensitivity troponin I (hs-cTnI). Figure C shows the relationship between the monocyte-to-neutrophil ratio (MNR) and cardiac tamponade.
These statistical analyses were based on two-sided tests.

3.6. Monocyte-to-neutrophil ratio in peripheral blood

Since macrophages, but not neutrophils, were the significant infiltrate in the hearts of cardiac tamponade cases, unlike in myocardial infarction cases, the monocyte-to-neutrophil ratio (MNR) in peripheral blood was examined. A significant increase was observed in the MNR in patients with cardiac tamponade complications (Fig. 5C). Thus, the MNR was increased in ATAAD with cardiac tamponade.

4. Discussion

Shock is classified into various types: Hemodynamic failure due to cardiac tamponade must be clearly distinguished from cardiogenic shocks, such as myocardial infarction, because cardiac tamponade represents obstructive shock that is due to decreased venous return and/or excessive afterload caused by anatomical damage [9]. Obstructive shock is a state of shock with tissue hypoxia in all organ systems due to a critical decrease in cardiac output and systemic oxygen supply, with a sudden decrease in cardiac output and blood pressure as common clinical features [10].

In the present study, we examined the histopathological findings of a case with a clear history of cardiac tamponade complication from the onset of ATAAD and the laboratory data for a cohort of 70 patients with ATAAD. High-sensitivity troponin I was significantly elevated with scattered contraction band necrosis in cardiac tamponade associated with ATAAD. Cardiac troponin is known to reflect not only myocardial ischemia, with dissection of the coronary artery entry or occlusion by a flap, but also abnormalities in the myocardial oxygen supply–demand balance [11]; obstructive shock was thought to be a contributing factor. These responses suggested that elevated troponin led to a poor prognosis in ATAAD [4,12]. Although contraction bands are also seen in artifacts, in this case they were scattered with C9, which was positive at the time of myocardial injury [13].

Acute Stanford type A aortic dissection and elevated troponin I are associated with elevated serum or myocardium CCL2 expression [14,15]. In this study, widespread CCL2 expression with VEGF-C and MMP9 expression was observed in macrophages at the site and tip of the dissociation, as well as in cardiomyocytes. Unexpectedly, in an autopsy case with a cardiac tamponade complication, the majority of macrophages were found to be positive for CD163 and CCL22. Such macrophages were identified as M2-like macrophages, which are thought to stabilize dissociated tissue [7,16]. Vascular endothelial growth factor is generally a vascularizing factor, although VEGF-C is important for the formation of granulation tissue and processing of necrotic tissue [17]. Matrix metalloproteinase 9 promotes cell migration and plays an important role in tissue repair [18–20] with the promotion of vascular proliferation by VEGF-C [21]. However, tissue repair mechanisms through these expressions may lead to a temporary weakening of tissue structures [22]. Aortic dissection is thought to be initiated by M1-like macrophages [23]. However, dissection is caused by repeated tissue damage and repair, constant force, and a predisposition to connective tissue abnormalities [24]. M2-like macrophages exhibit potent anti-inflammatory activity and play an important role in wound healing by regulating M1-like macrophages [8]. In particular, CD163-positive macrophages are responsible for processing hemoglobin as well as directly inducing anti-inflammatory cytokine secretory signals [25].

Of the laboratory data generally associated with acute myocardial damage, mean values for CK and WBC did not significantly differ between ATAAD patients with and without cardiac tamponade, while mean values of AST and LD were significantly elevated. Therefore, it was necessary to consider causes other than myocardial damage for the elevated AST and LD levels. Aspartate aminotransferase as an indicator of organ damage [26], and LDH as an indicator of biological reactions due to thrombolysis [27], were found to be significantly increased in cardiac tamponade cases. The cause appears to be the effect of severe organ damage and the presence of

an extensive false lumen. Furthermore, we found that the AST/LD ratio correlated with troponin I. This suggested that patients with organ damage and without thrombosis in a false lumen were more prone to the complication of cardiac tamponade. It was also thought that patients with cardiac tamponade have a longer cycle of damage and repair because of wide dissection in the vicinity of the heart. Because monocytes are required for repair, the blood MNR was found to be significantly elevated and M2-like macrophages may have infiltrated the lesion.

Macrophage aggregation in arterial lesions is associated with an increase in peripheral blood monocytes [28,29]. In an animal model of angiotensin II–induced aortic dissection, vascular accumulation of M1 macrophages was initially observed but these cells were replaced by M2 macrophages in the chronic phase [30]. Although the MNR is often discussed in terms of tumor progression [31] this may be due to the similarity of the tissue damage repair environment with the tumor microenvironment, which includes the proliferation of various cell types such as macrophages and angiogenesis.

In the present study, HDC, a histidine-converting enzyme that implies histamine expression along with CCL2, was identified in the lesions. Histamine is thought to promote the migration of CCL2 monocytes into tissues [32] and also enhances tissue healing and phagocytosis of macrophages and dendritic cells [33]. In addition, CCL22 cooperates with CCL2 to promote differentiation into M2-like macrophages [15,34,35]. In myocardium, the CCL2-induced migration of macrophages to the heart has been suggested to be associated with a blood pressure response or inflammation [36]. It was speculated that the various mechanisms involved in this transition from monocytes to macrophages may be one of the causes of the development of ATAAD with cardiac tamponade by making the aortic wall vulnerable and affecting blood hemodynamics.

This study has several limitations. First, the sample size was relatively small. In addition, it was a single-center study. Third, because it was a retrospective study, some values were missing, and laboratory data were collected only at the time of admission. However, at present, few studies have examined the characteristics of cardiac tamponade associated with aortic dissection, which we consider to be significant. It would therefore be beneficial to accumulate more such data in future.

5. Conclusions

In the present study, cardiac tamponade complications in ATAAD patients showed an association with an increased hs-cTnI level and were accompanied by elevated MNR via the expression of CCL2 and histamine. These observations may be associated with macrophage migration, suggesting an important role for M2-like macrophages in the development of a cardiac tamponade complication in ATAAD. Correlation with an elevated hs-cTnI level and LD/AST ratio also suggest an association of cardiac tamponade and ATAAD with the presence of extensive, communicating false lumens.

Ethics statement

This study was conducted in accordance with the Declaration of Helsinki and the Ethics Guidelines for Clinical Research issued by Japan's Ministry of Health, Labor and Welfare. The protocol of this study was approved by the Research Ethics Committee of the Kitakyushu City Hospital Organization (permission number: 202112001). Informed consent of patients was obtained through an opt-out methodology or written consent. Information on the research was made public on the Kitakyushu City Hospital Organization website, and the opportunity for the research subjects to refuse participation was guaranteed.

Funding

The authors did not receive any specific grant from funding agencies in the public, commercial or not-for-profit sectors.

Declaration of competing interest

The authors declare that they have no known competing financial interests or personal relationships that could have appeared to influence the work reported in this paper.

Acknowledgments

The authors would like to thank Yoshikazu Harada, Hana Nishimura, Rie Soeda, Yumiko Igawa, Fusa Murayama, Sayumi Kimura, and Miyo Kimura for their expert technical assistance.

References

[1] T. Yamaguchi, M. Nakai, T. Yano, M. Matsuyama, H. Yoshino, Y. Miyamoto, et al., Population-based incidence and outcomes of acute aortic dissection in Japan, Eur Heart J Acute Cardiovasc Care 10 (2021) 701–709.

[2] P.G. Hagan, C.A. Nienaber, E.M. Isselbacher, D. Bruckman, D.J. Karavite, P.L. Russman, et al., The international registry of acute aortic dissection (IRAD): new insights into an old disease, JAMA 283 (2000) 897–903.

[3] Y. Ren, S. Huang, Q. Li, C. Liu, L. Li, J. Tan, et al., Prognostic factors and prediction models for acute aortic dissection: a systematic review, BMJ Open 11 (2021), e042435.

[4] S. Kimura, S. Shimajiri, H. Sato, T. Araki, A. Sato, T. Nakayama, Recent trends in acute aortic dissection and the diagnostic potential of high-sensitivity troponin I, The Journal of Japanese Society of Laboratory Medicine 70 (2022) 653–658 (in Japanese).

[5] E. Bossone, R. Gorla, T.M. LaBounty, T. Suzuki, D. Gilon, C. Strauss, et al., Presenting systolic blood pressure and outcomes in patients with acute aortic dissection, J. Am. Coll. Cardiol. 71 (2018) 1432–1440.
[6] E.M. Isselbacher, J.E. Cigarroa, K.A. Eagle, Cardiac tamponade complicating proximal aortic dissection. Is pericardiocentesis harmful? Circulation 90 (1994) 2375–2378.
[7] X. Wang, H. Zhang, L. Cao, Y. He, A. Ma, W. Guo, The role of macrophages in aortic dissection, Front. Physiol. 11 (2020) 54.
[8] P.J. Murray, T.A. Wynn, Protective and pathogenic functions of macrophage subsets, Nat. Rev. Immunol. 11 (2011) 723–737.
[9] T. Standl, T. Annecke, I. Cascorbi, A.R. Heller, A. Sabashnikov, W. Teske, The nomenclature, definition and distinction of types of shock, Dtsch Arztebl Int 115 (2018) 757–768.
[10] K. Sasaguri, H. Irie, T. Imaizumi, N. Kamochi, Y. Egashira, J. Nojiri, et al., Retrospective analysis of contrast-enhanced computed tomographic findings related to obstructive shock due to ascending aortic dissection, J. Comput. Assist. Tomogr. 36 (2012) 60–66.
[11] G. Li, X.W. Wu, W.H. Lu, J. Cheng, X.Y. Wu, R. Ai, et al., High-sensitivity cardiac troponin T: a biomarker for the early risk stratification of type-A acute aortic dissection? Arch Cardiovasc Dis 109 (2016) 163–170.
[12] F. Vagnarelli, A. Corsini, G. Bugani, M. Lorenzini, S. Longhi, M.L. Bacchi Reggiani, et al., Troponin T elevation in acute aortic syndromes: frequency and impact on diagnostic delay and misdiagnosis, Eur Heart J Acute Cardiovasc Care 5 (2016) 61–71.
[13] M.A. Ferreira, H.E. Owen, A.J. Howie, High prevalence of acute myocardial damage in a hospital necropsy series, shown by C9 immunohistology, J. Clin. Pathol. 51 (1998) 548–551.
[14] F. Del Porto, C. di Gioia, L. Tritapepe, L. Ferri, M. Leopizzi, I. Nofroni, et al., The multitasking role of macrophages in Stanford type A acute aortic dissection, Cardiology 127 (2014) 123–129.
[15] Z. Kaya, S. Göser, S.J. Buss, F. Leuschner, R. Ottl, J. Li, et al., Identification of cardiac troponin I sequence motifs leading to heart failure by induction of myocardial inflammation and fibrosis, Circulation 118 (2008) 2063–2072.
[16] S. Kimura, H. Noguchi, U. Nanbu, K.Y. Wang, Y. Sasaguri, T. Nakayama, Relationship between CCL22 expression by vascular smooth muscle cells and macrophage histamine receptors in atherosclerosis, J. Atherosclerosis Thromb. 25 (2018) 1240–1254.
[17] J. Asai, H. Takenaka, S. Hirakawa, J. Sakabe, A. Hagura, S. Kishimoto, et al., Topical simvastatin accelerates wound healing in diabetes by enhancing angiogenesis and lymphangiogenesis, Am. J. Pathol. 181 (2012) 2217–2224.
[18] A.H. Webb, B.T. Gao, Z.K. Goldsmith, A.S. Irvine, N. Saleh, R.P. Lee, et al., Inhibition of MMP-2 and MMP-9 decreases cellular migration, and angiogenesis in vitro models of retinoblastoma, BMC Cancer 17 (2017) 434.
[19] C. Legrand, C. Gilles, J.M. Zahm, M. Polette, A.C. Buisson, H. Kaplan, et al., Airway epithelial cell migration dynamics. MMP-9 role in cell-extracellular matrix remodeling, J. Cell Biol. 146 (1999) 517–529.
[20] C.A. Meschiari, M. Jung, R.P. Iyer, A. Yabluchanskiy, H. Toba, M.R. Garrett, et al., Macrophage overexpression of matrix metalloproteinase-9 in aged mice improves diastolic physiology and cardiac wound healing after myocardial infarction, Am. J. Physiol. Heart Circ. Physiol. 314 (2018) H224–H235.
[21] M. Sano, T. Sasaki, S. Hirakawa, J. Sakabe, M. Ogawa, S. Baba, et al., Lymphangiogenesis and angiogenesis in abdominal aortic aneurysm, PLoS One 9 (2014), e89830.
[22] S. Katsuda, Y. Okada, Y. Okada, K. Imai, I. Nakanishi, Matrix metalloproteinase-9 (92-kd gelatinase/type IV collagenase equals gelatinase B) can degrade arterial elastin, Am. J. Pathol. 145 (1994) 1208–1218.
[23] Q. Wang, Z. Chen, X. Peng, Z. Zheng, A. Le, J. Guo, et al., Neuraminidase 1 exacerbating aortic dissection by governing a pro-inflammatory program in macrophages, Front Cardiovasc Med 8 (2021), 788645.
[24] I. Sen, Y.M. Erben, C. Franco-Mesa, R.R. DeMartino, Epidemiology of aortic dissection, Semin. Vasc. Surg. 34 (2021) 10–17.
[25] S.K. Moestrup, H.J. Møller, CD163: a regulated hemoglobin scavenger receptor with a role in the anti-inflammatory response, Ann. Med. 36 (2004) 347–354.
[26] M. Wen, Y. Han, J. Ye, G. Cai, W. Zeng, X. Liu, et al., Peri-operative risk factors for in-hospital mortality in acute type A aortic dissection, J. Thorac. Dis. 11 (2019) 3887–3895.
[27] M.V. Gavalas, A. Breskin, M. Yuzefpolskaya, A. Eisenberger, F. Castagna, R.T. Demmer, et al., Discriminatory performance of positive urine hemoglobin for detection of significant hemolysis in patients with continuous-flow left ventricular assist devices, J. Heart Lung Transplant. 36 (2017) 59–63.
[28] F.K. Swirski, M.J. Pittet, M.F. Kircher, E. Aikawa, F.A. Jaffer, P. Libby, et al., Monocyte accumulation in mouse atherogenesis is progressive and proportional to extent of disease, Proc. Natl. Acad. Sci. U.S.A. 103 (2006) 10340–10345.
[29] P. Dutta, G. Courties, Y. Wei, F. Leuschner, R. Gorbatov, C.S. Robbins, et al., Myocardial infarction accelerates atherosclerosis, Nature 487 (2012) 325–329.
[30] J.P. Moore, A. Vinh, K.L. Tuck, S. Sakkal, S.M. Krishnan, C.T. Chan, et al., M2 macrophage accumulation in the aortic wall during angiotensin II infusion in mice is associated with fibrosis, elastin loss, and elevated blood pressure, Am. J. Physiol. Heart Circ. Physiol. 309 (2015) H906–H917.
[31] Y. Guan, F. Xu, J. Tian, Y. Wang, N. Guo, Z. Wan, et al., Prognostic value of circulating tumor cells and immune-inflammatory cells in patients with renal cell carcinoma, Urol. Oncol. 40 (2022) 167.e21–167.e32.
[32] S. Kimura, K.Y. Wang, A. Tanimoto, Y. Murata, Y. Nakashima, Y. Sasaguri, Acute inflammatory reactions caused by histamine via monocytes/macrophages chronically participate in the initiation and progression of atherosclerosis, Pathol. Int. 54 (2004) 465–474.
[33] P. Dutta, M. Nahrendorf, Regulation and consequences of monocytosis, Immunol. Rev. 262 (2014) 167–178.
[34] S. Kimura, U. Nanbu, H. Noguchi, Y. Harada, K. Kumamoto, Y. Sasaguri, et al., Macrophage CCL22 expression in the tumor microenvironment and implications for survival in patients with squamous cell carcinoma of the tongue, J. Oral Pathol. Med. 48 (2019) 677–685.
[35] S. Kimura, H. Noguchi, K. Yoshida, H. Sato, U. Nanbu, D. Niino, et al., Relationship of histamine expression with chemokine balance in the tumor microenvironment of squamous cell carcinoma of the tongue, Head Neck 44 (2022) 1554–1562.
[36] J.Z. Shen, J. Morgan, G.H. Tesch, P.J. Fuller, M.J. Young, CCL2-dependent macrophage recruitment is critical for mineralocorticoid receptor-mediated cardiac fibrosis, inflammation, and blood pressure responses in male mice, Endocrinology 155 (2014) 1057–1066.